Science Advances
AAAS

advances.sciencemag.org/cgi/content/full/5/8/eaav8463/DC1

Supplementary Materials for

BRAF inhibitors promote intermediate BRAF(V600E) conformations and binary interactions with activated RAS

Ruth Röck, Johanna E. Mayrhofer, Omar Torres-Quesada, Florian Enzler, Andrea Raffeiner, Philipp Raffeiner, Andreas Feichtner, Roland G. Huber, Shohei Koide, Susan S. Taylor, Jakob Troppmair, Eduard Stefan*

*Corresponding author. Email: eduard.stefan@uibk.ac.at

Published 14 August 2019, *Sci. Adv.* **5**, eaav8463 (2019)
DOI: 10.1126/sciadv.aav8463

This PDF file includes:

Table S1. Used expression constructs, materials, and cell lines.

Used constructs	SOURCE	IDENTIFIER
PPI REPORTER		
RAF		
pcDNA3-BRAF-RLucF1	This paper	N/A
pcDNA3-BRAF-RLucF2	This paper	N/A
pcDNA3-BRAF(V600E)-RLucF1	This paper	N/A
pcDNA3-BRAF(V600E)-RLucF2	This paper	N/A
pcDNA3-RLucF1-BRAF	This paper	N/A
pcDNA3-RLucF1-BRAF(V600E)	This paper	N/A
pcDNA3-BRAF(R509H)-RLucF1	This paper	N/A
pcDNA3-BRAF(R509H)-RLucF2	This paper	N/A
pcDNA3-BRAF(R509H/V600E)-RLucF1	This paper	N/A
pcDNA3-BRAF(R509H/V600E)-RLucF2	This paper	N/A
pcDNA3-BRAF(R166A)-RLucF1	This paper	N/A
pcDNA3-BRAF(R188A)-RLucF1	This paper	N/A
pcDNA3-BRAF(R166A/R188A)-RLucF1	This paper	N/A
pcDNA3-BRAF(R166A/V600E)-RLucF1	This paper	N/A
pcDNA3-BRAF(R188A/V600E)-RLucF1	This paper	N/A
pcDNA3-BRAF(417-766)-RLucF1	This paper	N/A
pcDNA3-BRAF(417-766)-RLucF2	This paper	N/A
pcDNA3-BRAF-RBD-RLucF1	This paper	N/A
pcDNA3-BRAF-RBD-RLucF2	This paper	N/A
pcDNA3-CRAF-RLucF1	This paper	N/A
pcDNA3-CRAF-RLucF2	This paper	N/A
pcDNA3-CRAF(R89A)-RLucF2	This paper	N/A
pcDNA3-CRAF-RBD-RLucF1	This paper	N/A
pcDNA3-CRAF-RBD-RLucF2	This paper	N/A
pcDNA3-CRAF-NL	This paper	N/A
pcDNA3-CRAF(R89A)-NL	This paper	N/A
RAS		
pcDNA3-HRAS-RLucF1	This paper	N/A
pcDNA3-HRAS-RLucF2	This paper	N/A
pcDNA3-HRAS(G12V)-RLucF1	This paper	N/A
pcDNA3-HRAS(G12V)-RLucF2	This paper	N/A
pcDNA3-NRAS-RLucF1	This paper	N/A
pcDNA3-NRAS-RLucF2	This paper	N/A
pcDNA3-NRAS(G12V)-RLucF1	This paper	N/A
pcDNA3-NRAS(G12V)-RLucF2	This paper	N/A
pcDNA3-FLAG-HRAS	This paper This	N/A
pcDNA3-FLAG-HRAS(G12V)	paper	N/A
pcDNA3-KRAS-RLucF1	This paper	N/A
pcDNA3-KRAS-RLucF2	This paper	N/A
pcDNA3-KRAS(G12V)-RLucF1	This paper	N/A
pcDNA3-KRAS(G12V)-RLucF2	This paper	N/A
VARIOUS		
pcDNA3-RIIb-RLucF1	This paper	N/A
pcDNA3-RIIb-RLucF2	This paper	N/A
pcDNA3-MAX-RLucF2	This paper	N/A
pcDNA3-RLuc	This paper	N/A
pcDNA3-YFP	This paper	N/A

KinCon REPORTER

RAF

pcDNA3-RLucF1-BRAF-RLucF2	This paper	N/A
pcDNA3-RLucF1-BRAF(G469A)-RLucF2	This paper	N/A
pcDNA3-RLucF1-BRAF(D594G)-RLucF2	This paper	N/A
pcDNA3-RLucF1-BRAF(V600E)-RLucF2	This paper	N/A
pcDNA3-RLucF1-BRAF(V600K)-RLucF2	This paper	N/A
pcDNA3-RLucF1-BRAF(K601E)-RLucF2	This paper	N/A
pcDNA3-RLucF1-BRAF(T529I)-RLucF2	This paper	N/A
pcDNA3-RLucF1-BRAF(T529M)-RLucF2	This paper	N/A
pcDNA3-RLucF1-BRAF(S365A)-RLucF2	This paper	N/A
pcDNA3-RLucF1-BRAF(S729A)-RLucF2	This paper	N/A
pcDNA3-RLuc-F1-BRAF(S365A/V600E)-RLucF2	This paper	N/A
pcDNA3-RLuc-F1-BRAF(S729A/V600E)-RLucF2	This paper	N/A
pcDNA3-RLucF1-BRAF(T529I/V600E)-RLucF2	This paper	N/A
pcDNA3-RLucF1-BRAF(T529M/V600E)-RLucF2	This paper	N/A

PEPTIDE TAGGED PROTEINS

pcDNA3-HA-BRAF	This paper	N/A
pcDNA3-HA-BRAF(V600E)	This paper	N/A
pcDNA3-FLAG-BRAF	This paper	N/A
pcDNA3-FLAG-BRAF(V600E)	This paper	N/A
pcDNA3-FLAG-BRAF(R509H)	This paper	N/A
pcDNA3-FLAG-BRAF(R509H/V600E)	This paper	N/A
pcDNA3-FLAG-BRAF(R188A)	This paper	N/A
pcDNA3-FLAG-BRAF(R188A/V600E)	This paper	N/A
pcDNA3-V5-CRAF	This paper	N/A
pcDNA3-V5-CRAF(R89A)	This paper	N/A
pcDNA3-HA-HRAS	This paper	N/A
pcDNA3-HA-HRAS(G12V)	This paper	N/A
pcDNA3-NS1-YFP	This paper	N/A
pcDNA3-NS1neg-YFP	This paper	N/A

ANITBODY	SOURCE	IDENTIFIER
C-RAF polyclonal	Cell Signaling	9422S
B-RAF	Santa Cruz	F-7: sc-5284, C-19: sc-166
FLAG	Sigma-Aldrich	F3165
GFP	Roche	11814460001
HA-tag	Covance	MMS-10P
mAB anti RLuc-F1	Millipore	MAB4410
mAB anti RLuc-F2	Millipore	MAB4400
pan RAS Antibody (RAS10)	Thermo Scientific	MA1-012X
P-ERK1/2 p44/P42 MAPK	Cell Signaling	9101
ERK1/2 p44/p42 MAPK	Cell Signaling	4696S
P-MEK1/2	Cell Signaling	9154
MEK1/2	Cell Signaling	4694
PKA-RIIb	BD Biosciences	610626
V5	Invitrogen	R96025

REAGENTS	SOURCE	IDENTIFIER
PLASMID DNA TRANSFECTION		
Transfectin reagent	Biorad	1703352
jetPRIME reagent	Polyplus-transfection	114-07
SELECTION MARKER		
Ampicillin	Sigma-Aldrich	A9518-25G
Hygromycin B	Thermo Scientific	10687-010
Zeocin	Invitrogen	R25001
KINASE INHIBITORS		
Vemurafenib PLX4032	MedChem Express	HY-12057
PLX8394	MedChem Express	HY-18972
Encorafenib LGX818	MedChem Express	HY-15605
Dabrafenib GSK2118436A	Selleckchem	S2807
AZ628	Selleckchem	S2746
GDC0879	Selleckchem	S1104
LY3009120	Selleckchem	S7842
TAK632	Selleckchem	S7291
Selumetinib AZD6244	Selleckchem	S1008
Refametinib BAY86-9766	MedChem Express	HY-102156

CELL LINES	SOURCE	IDENTIFIER
HEK293	ATCC	N/A
SW480	ATCC	N/A
A375	ATCC	N/A
STABLE CELL LINES		
SW480 RBD BRAF-RLucF1, HRAS(G12V)-RLucF2	This paper	N/A
SW480 BRAF-RLucF1, HRAS(G12V)-RLucF2	This paper	N/A
SW480 BRAF(V600E)-RLucF1, HRAS(G12V)-RLucF2	This paper	N/A

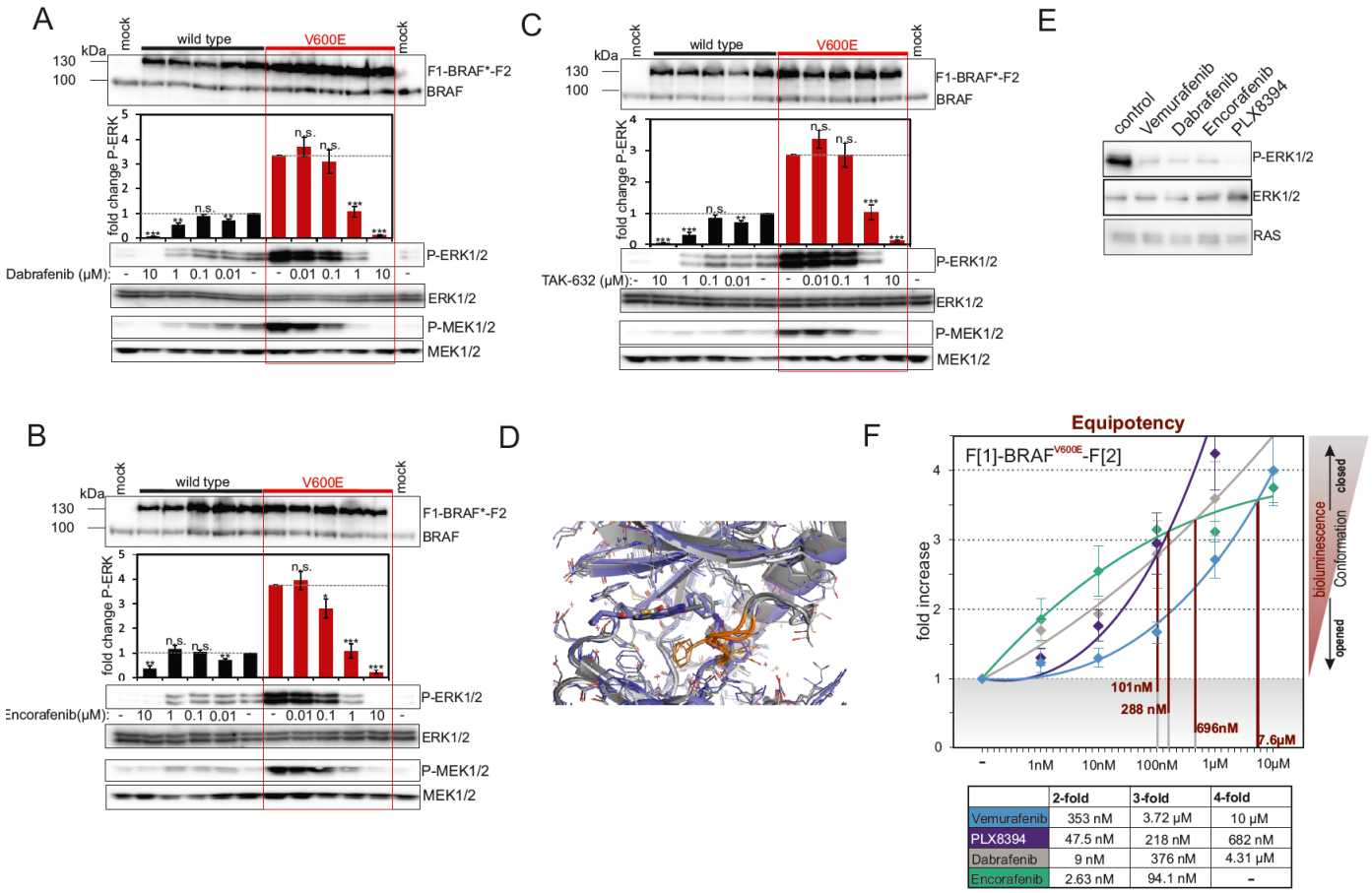

	2-fold	3-fold	4-fold
Vemurafenib	353 nM	3.72 μM	10 μM
PLX8394	47.5 nM	218 nM	682 nM
Dabrafenib	9 nM	376 nM	4.31 μM
Encorafenib	2.63 nM	94.1 nM	-

Fig. S1. BRAF KinCon reporter activities and BRAF profiling. (A-C) Impact of BRAF KinCon reporter expression (for 48h) and 1h dose-dependent BRAFi inhibitor exposure on ERK1/2 and MEK1/2 phosphorylations (±SEM; n=4 independent experiments). Student's t-test was used to evaluate statistical significance. Confidence level: *P<0.05, **P<0.01, ***P<0.001. **(D)** Shown are the structural binding characteristics of TAK632 (in purple) when compared with LY3009120 and AZ628 (in grey). **(E)** Impact of 1μM/1h BRAFi exposure on P-ERK signals (representative experiment, A375 melanoma cell line). **(F)** Impact of indicated BRAFi on the closing of BRAF-V600E KinCon reporters. Data from Figs. 1E and 2A have been used and conformation closing curves have been generated. The dose-dependent effects of vemurafenib, PLX8394, dabrafenib, and encorafenib on the BRAF-V600E KinCon reporters were normalized on the untreated settings. For each BRAFi polynomial regression trend lines are presented. Equi-potencies of pairs of BRAFi are indicated in the graph in red. In the table we list concentrations of equi-potencies for BRAFi for fold-changes of the KinCon conformations.

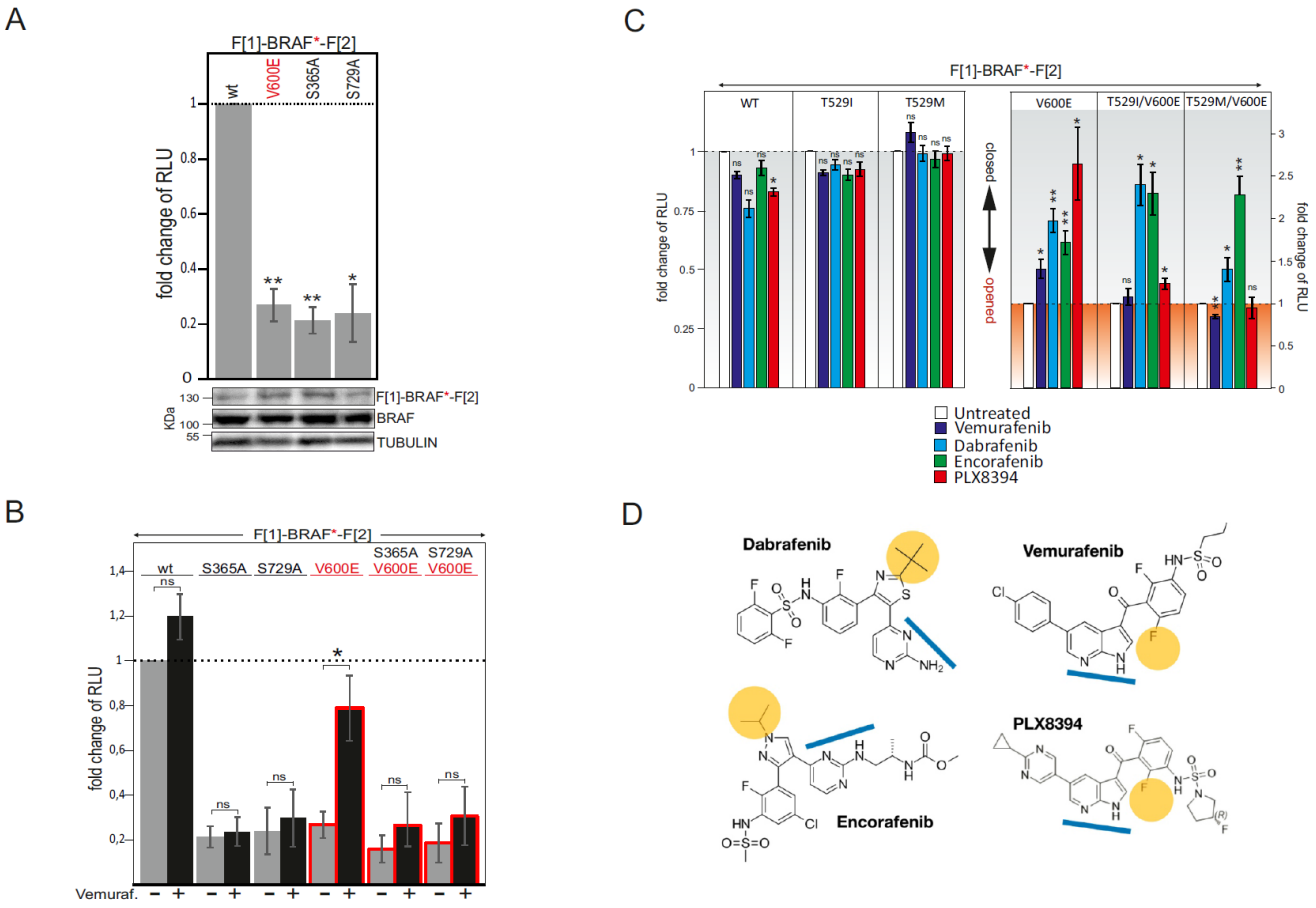

Fig. S2. Impact of defined kinase mutations on BRAF KinCon reporter dynamics. (A) Following transient expression of indicated KinCon reporter for 24h, we performed bioluminescence analyses. Quantification is shown from n=4 independent experiments; ±SEM. **(B)** Following transient expression of indicated KinCon reporter for 24h we treated cells for 1 h with 1µM Vemurafenib followed by *R*luc PCA analyses. Quantification is shown from n=3 independent experiments; ±SEM. **(C)** Shown is the impact of gatekeeper mutations T529M and T529I in combinations with V600E on KinCon reporter dynamics upon BRAFi treatment (1h, 1µM). Quantification is shown from n=5 independent experiments; ±SEM. **(D)** Comparison of structure features of indicated BRAFi relevant for gatekeeper mutation interactions. The hydrophobic groups are indicated in yellow, the hinge binding motif is indicated as a blue bar. Confidence level: *P<0.05, **P<0.01, ***P<0.001.

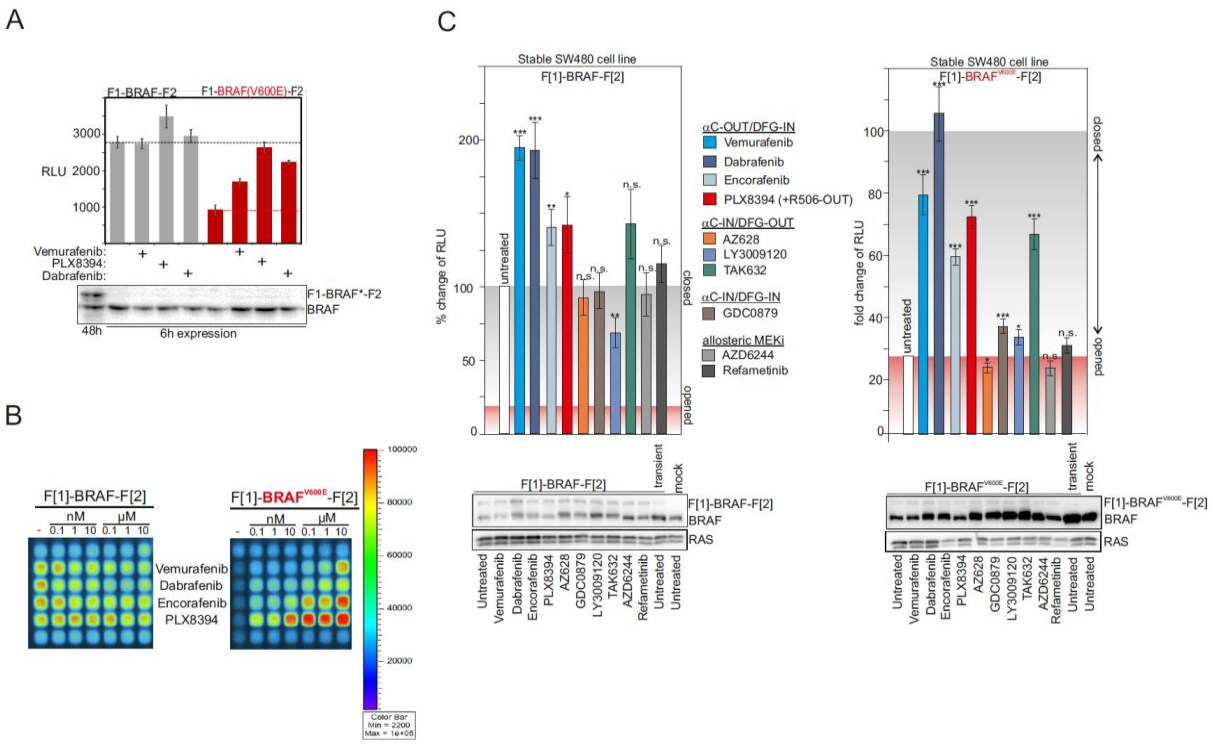

Fig. S3. BRAF KinCon reporter dynamics. (A) Following transient expression of indicated KinCon reporter for 6h and 24h we treated HEK293 cells with indicated BRAFi (1 µM; 1h). Shown is a representative experiment of n=3. **(B)** Bioluminescence imaging of detached HEK293 cells expressing indicated KinCon reporters in sections of a 1536-well plate (pseudo-color scaling of emitted RLU). **(C)** Impact of indicated BRAFi and MEKi on shown BRAF KinCon reporters stably expressed in SW480 cells (±SEM; n=5 independent experiments). Bioluminescence signals have been normalized to the reporter expression levels (ratios of endogenous BRAF/reporter; the $BRAF^{V600E}$ KinCon reporter signals are ~ 28% when compared to the wild type).

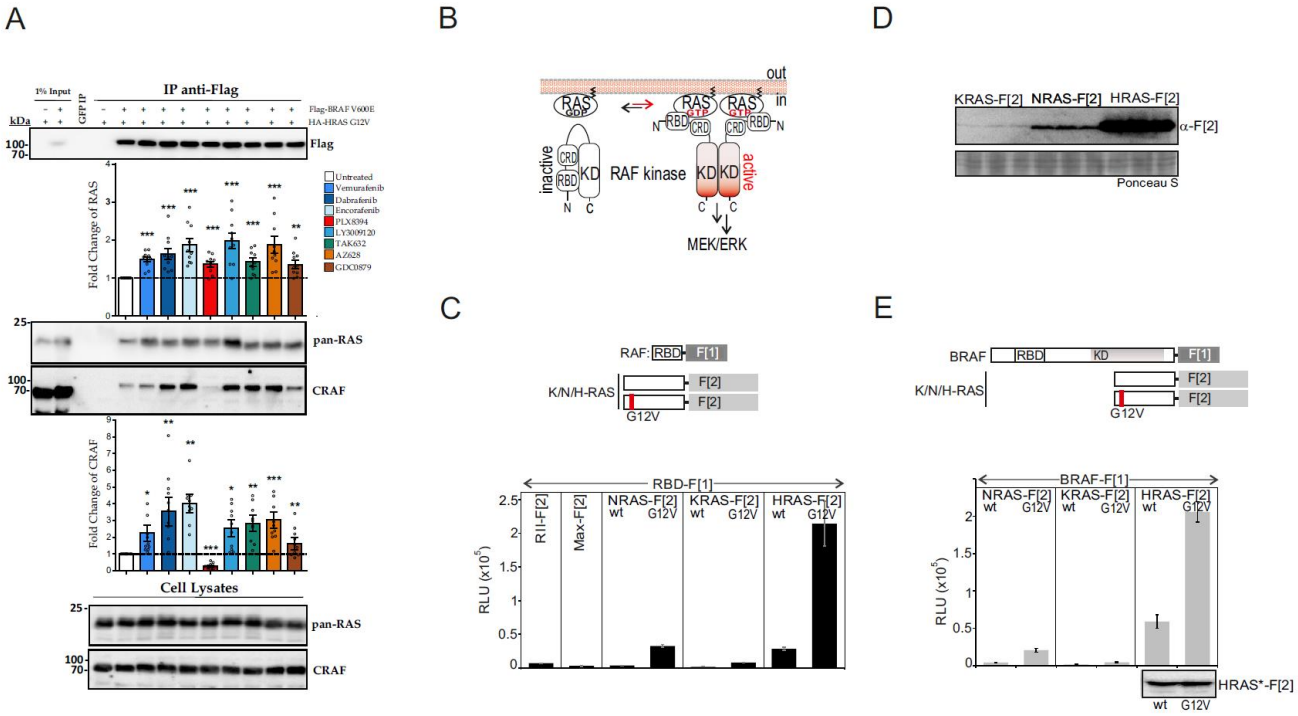

Fig. S4. Complex formation of RAS:BRAF and PPI reporter dynamics. (A) Shown are immunoprecipitations of transiently overexpressed flag-BRAF^{V600E} and HA-HRAS^{G12V} using flag-tag antibodies from HEK293 cells following 1h RAFi exposure (quantification is shown from n=10 independent experiments; ±SEM). **(B)** GDP/GTP exchange affects RAS:RAF complex formation and downstream signaling; RAS binding domain (RBD), Cysteine rich domain (CRD), kinase domain (KD). **(C)** Following co-expression of pairs of either full-length RAS isoforms/mutants, Max, and RII with the RAS binding domain (RBD) tagged with indicated *R*luc PCA fragments we determined bioluminescence signals (RLU) using the *R*luc-PCA as read out (±SD; representative of n=3). **(D)** Immunoblotting indicates differences of expression levels of indicated RAS isoforms tagged with *R*luc PCA -F[2]. **(E)** Following co-expression of *R*luc-PCA fragment tagged pairs of RAS isoforms/mutants and full length BRAF we determined GTP-dependent PPIs (±SD; representative experiment of n=3 independent experiments). Student's t-test was used to evaluate statistical significance. Confidence level: *P<0.05, **P<0.01, ***P<0.001.

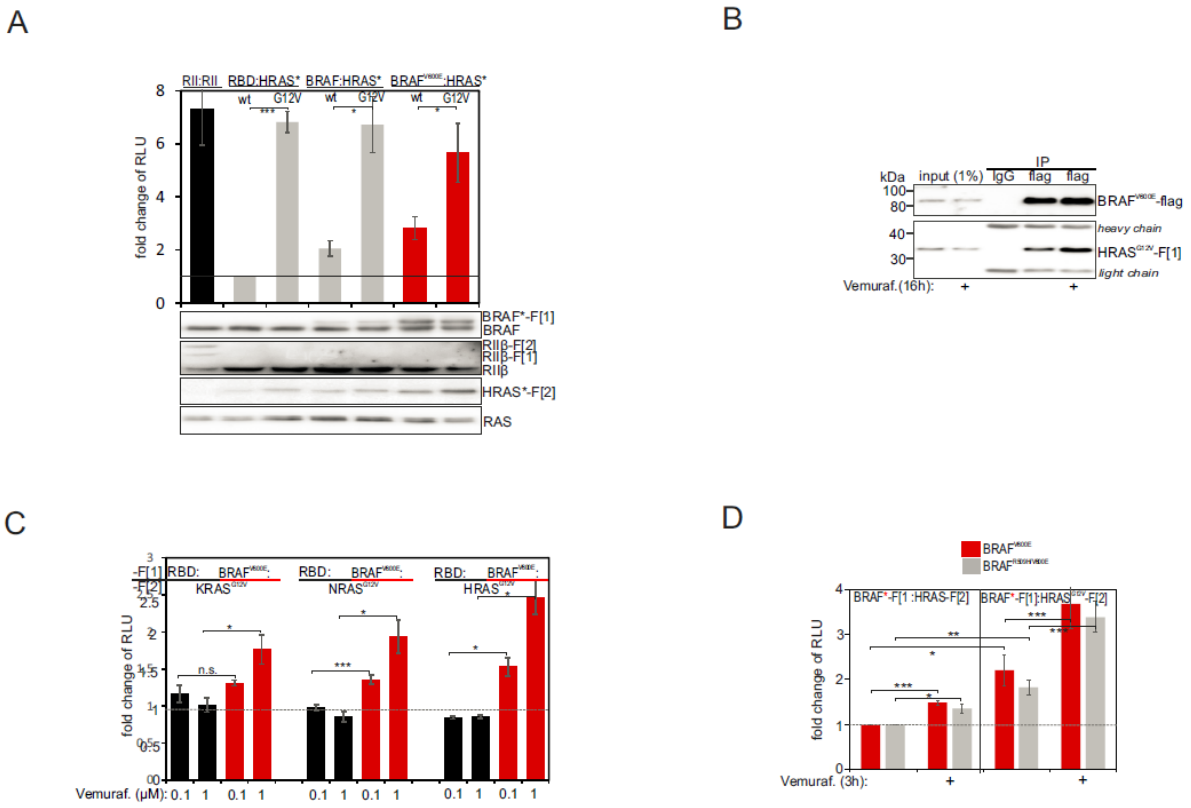

Fig. S5. Impact of vemurafenib on indicated PPIs. (A) Following co-expression of indicated *R*luc-PCA fragment tagged pairs in HEK293 cells PPI values have been determined (±SEM from n=4 independent experiments). **(B)** Co-immunoprecipitation of flag-tagged BRAF-V600E and HRASG12V-F[1] transiently expressed in HEK293 cells following treatments with vemurafenib (10 µM, 16h; representative of n=3). **(C)** Following co-expression of PPI reporter combinations of BRAF, RBD, H-, N-, and K-RAS we treated cells with increasing vemurafenib concentrations (0.1 and 1 µM). Shown is the PPI analyses of n=3 independent experiments (HEK293, ±SEM; normalized either on 0,1 and/or 1 µM Vemurafenib treatment of RBD:RAS interactions). **(D)** Following integration of the R509H mutation (impairs RAF dimerization) into the PPI reporter construct BRAF-V600E we analyzed the effect of vemurafenib treatment on complex formation (1 µM, 3h, n=4 ind. experiments; ±SEM; HEK293). Student's t-test was used to evaluate statistical significance. Confidence level: *P<0.05, **P<0.01, ***P<0.001.

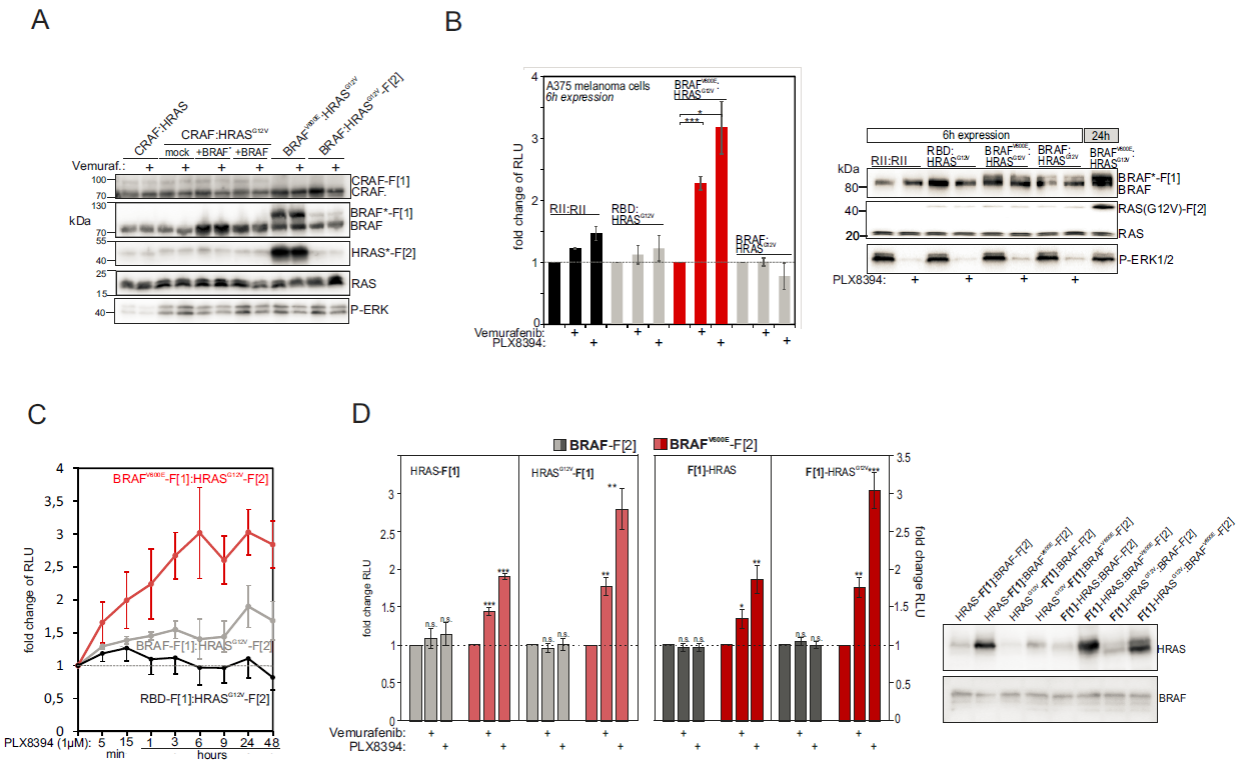

Fig. S6. Impact of BRAFi on binary RAS:RAF interactions. (A) representative expression analyses of PPI reporter as shown in Fig. 5C. **(B)** Following coexpression of indicated PPI reporters for 6 h and 24 h we treated A375 cells with PLX8394 and vemurafenib (1 µM; 3h). Shown are the PPI analyses of n=3 independent experiments (±SEM). **(C)** Time-dependent effects of PLX8394 exposure (1 µM) on the bioluminescence of SW480 cells stably expressing indicated PPI reporter pairs (n=4 ind. experiments, ±SEM). **(D)** Impact of vemurafenib or PLX8394 exposure (3h, 1 µM) on N or C terminal tagged HRAS *R*luc-PCA PPI reporter (n=4 ind. experiments, ±SEM). Student's t-test was used to evaluate statistical significance. Confidence level: *P<0.05, **P<0.01, ***P<0.001.

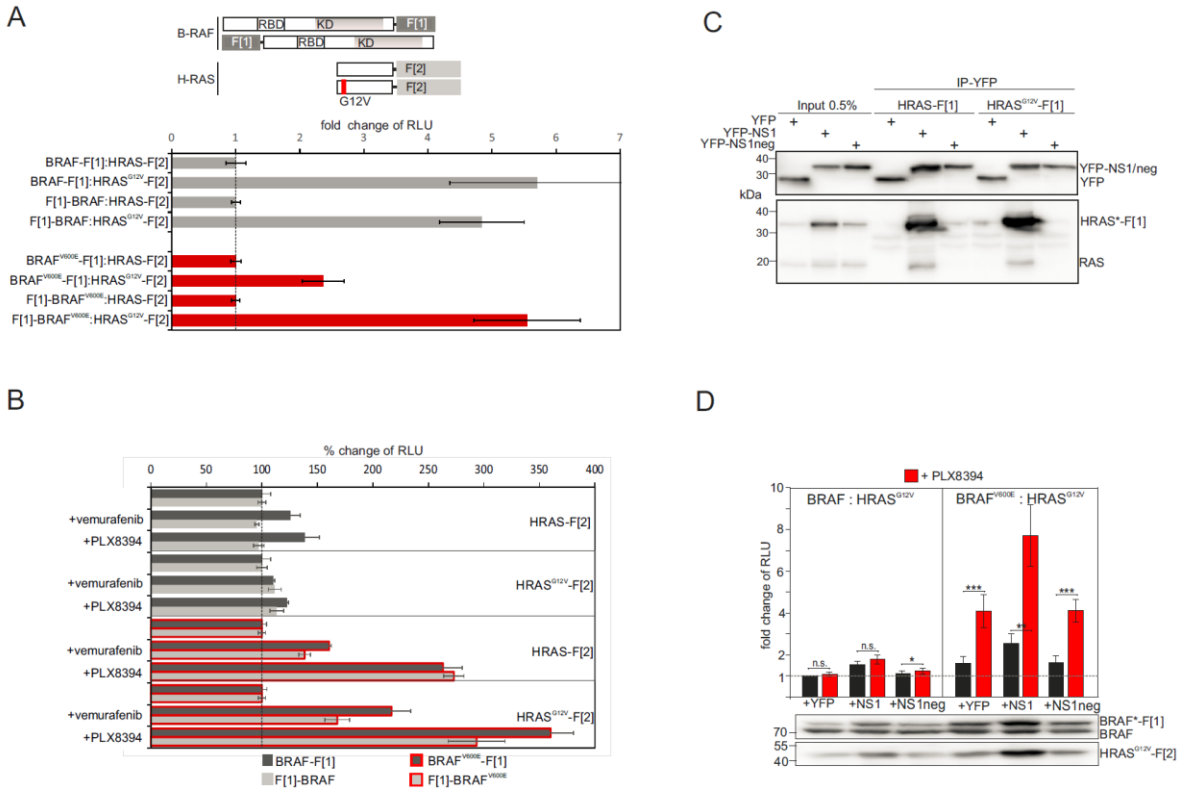

Fig. S7. PPI reporter dynamics and NS1 monobody IPs. (A) Schematic depiction of the PPI reporter constructs. Impact of the G12V mutation in HRAS on the binary interaction with either N- or C-terminally tagged BRAF using the *R*luc-PCA PPI reporter as read out (n=4 experiments, ±SD). **(B)** Impact of vemurafenib or PLX8394 exposure (3h, 1 µM) on indicated PPI reporter interactions (n=4 ind. experiments, ±SEM). **(C)** Shown are representative co-IP (of n=3 ind. exp.) of YFP or YFP-tagged hybrid proteins with endogenous RAS and *R*luc-PCA tagged HRAS. **(D)** PPI reporter analyses of transiently expressed reporter protein pairs following 3h treatment with PLX8394. Quantifications from n=5 independent experiments are shown (±SEM).

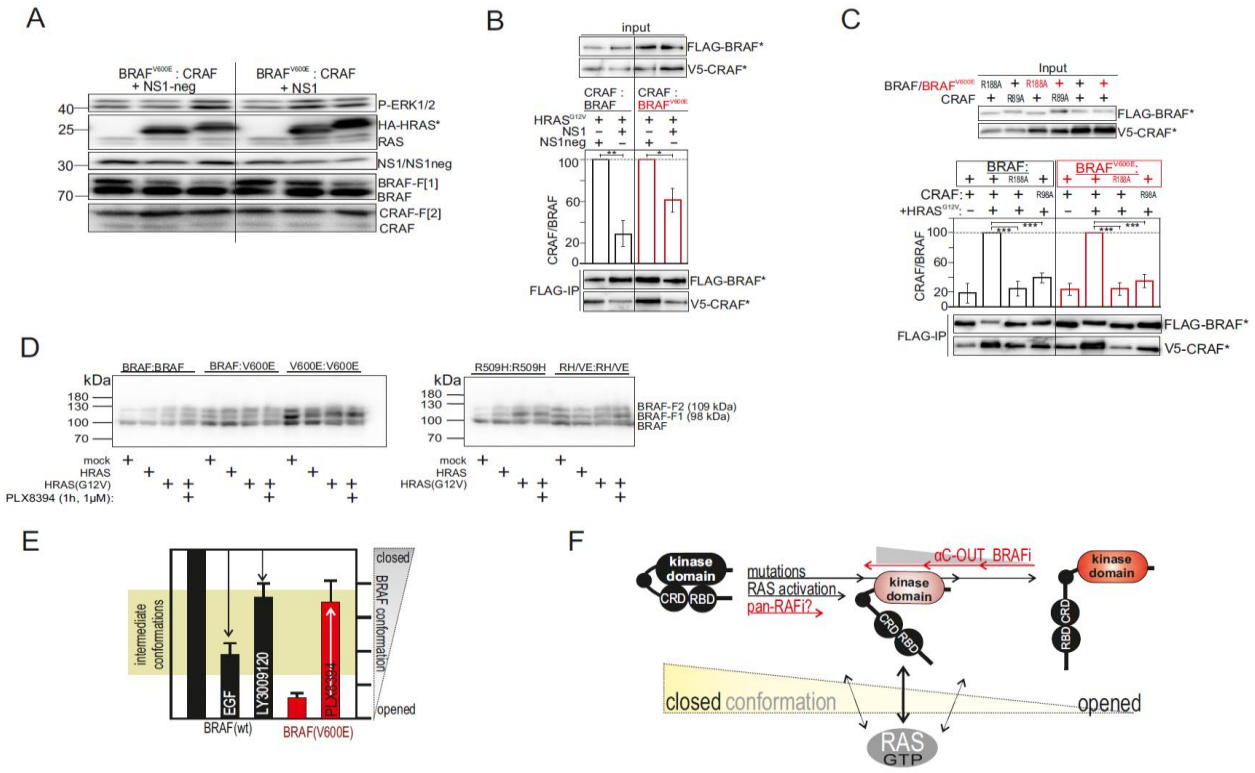

Fig. S8. Validation of PPI dynamics and impact of RAFi on RAF conformations. (A) Representative expression profiling of PPI reporter hybrid proteins following coexpression of NS1, NS1neg, and HRAS variants as shown in Fig. 6C. **(B)** IPs of indicated RAF variants from HEK293 cells are shown. Representative IP of n=4 independent experiments are shown (±SEM). **(C)** IPs of indicated RAF mutants from HEK293 cells. Representative IP of n=4 independent experiments are shown (±SD). **(D)** Representative expression profiling of PPI reporter hybrid proteins as presented in Fig. 6E. **(E)** Shown are the effects of EGF activation, V600E mutations, and BRAFi exposure on the formation of intermediate BRAF conformations. Data have been extracted from Fig. 1. **(F)** Detailed depiction of (1) and (2) from Fig. 6G (RAF dimer formation has been neglected). RAS-activation, dose-dependent BRAFi engagements (triangle; αC-OUT BRAFi and probably some pan-BRAFi), and BRAF mutations (class I, II or III) may have the potential to convert BRAF to intermediate kinase conformations showing elevated affinities for GTP-loaded RAS.